

ELECTRONIC SUPPLEMENTARY INFORMATION

Unraveling the local energetics of transport in a polymer ion conductor

Mark D. Lingwood, Zhiyang Zhang, Bryce E. Kidd, Kacey B. McCreary, Jianbo Hou, and Louis A. Madsen

Experimental

Sample Preparation

The perfluorosulfonate ionomer Nafion 117 CS (extruded, 1100 equivalent weight per sulfonate group) was obtained from E.I. DuPont (Wilmington, DE) in acid form. The membrane was cut into nine 4 mm × 4 mm pieces, which were stacked and loosely wrapped in polytetrafluoroethylene (PTFE) tape. The desired water uptake was obtained by soaking the sample in deionized water (or D₂O) then allowing water to evaporate until the mass of the sample reached the chosen range. The membrane stack was then blotted to remove excess moisture, tightly wrapped in polyethylene food sealing wrap, and placed into a custom-built 8 mm PTFE sample cell with low dead volume and excellent sealing characteristics.^{S1} Samples were equilibrated in the sample cell for 1–3 hr before measurement. After NMR experiments, the sample was removed and weighed again. After completing the entire set of experiments, the membrane was dried at 105 °C under vacuum for two days and weighed to obtain the dry mass. The mass after each NMR experiment ($mass_{wet}$) and the overall dry mass ($mass_{dry}$) were used to calculate the mass percent of water in the membrane through equation S1:

$$\text{water uptake} = \frac{mass_{wet} - mass_{dry}}{mass_{dry}} \times 100\% = \frac{mass_{water}}{mass_{dry}} \times 100\% \quad (S1)$$

Water uptake is converted to λ (moles of water / moles SO₃⁻) upon multiplying by the equivalent weight (1100 grams dry polymer / mole sulfonate group) and dividing by the molecular weight of water (18.01 grams water / mole) or D₂O. The error in λ based on mass uptakes and residual water in the dried membrane is estimated to be < +/- 0.5, with some reduction in error at low λ . We note that some debate in the literature exists regarding the meaning of “dry” Nafion. Based on a reputable study,^{S2} we conclude that our drying procedure leaves at most 0.2 wt% water ($\lambda < 0.2$) in the membrane so that we are confident in our significantly wider stated error bars.

Trifluoromethanesulfonic acid (triflic acid) was obtained from Fisher Scientific (USA). Aqueous solutions of triflic acid were made by placing an appropriate amount of water in a vial, adding an approximate amount of ice-bath-chilled triflic acid, then quickly sealing the vial. After allowing the mixture to stand for 10 min, the vials were weighed to obtain the mass of triflic acid. The mixtures were then transferred to 5 mm NMR tubes and quickly flame sealed in air. To alleviate convection effects during the NMR diffusion measurements, the 5 mm NMR tubes each contained 4 axial capillaries of 0.8 mm inner diameter and 1.0 mm outer diameter (Fisher Scientific). A solid resulted when equal amounts of triflic acid and water were mixed ($\lambda = 1.0$), due to the formation of triflic acid monohydrate, however liquid solutions could be created at λ below and above 1.0.

NMR Measurements

All NMR measurements were obtained using a Bruker Avance III widebore 400 MHz (9.4 T) NMR equipped with a Diff60 diffusion probe with exchangeable coil inserts (Bruker Biospin, Billerica, MA). Membrane diffusion was measured with either an 8 mm ¹H or 10 mm ²H coil, and the triflic acid solutions were measured with a 5 mm ¹H/¹⁹F coil. The pulsed-gradient stimulated echo (PGSTE) sequence was used to measure diffusion, with an effective gradient pulse length of $\delta = 2$ ms, gradient

pulse spacing of $\Delta = 50$ ms, and maximum gradient strengths ranging from $g = 28$ G/cm to $g = 1800$ G/cm. 16 gradient steps were applied, and the number of scans varied from 4 to 128 for adequate SNR. Diffusion was measured along the spectrometer magnetic field ($B_0 = z$) direction, and the membranes were oriented so that the extrusion striate was aligned with B_0 , and therefore diffusion was measured along the extrusion direction in these nearly isotropic samples.^{S1} A single symmetric NMR line was observed in all ^1H and ^{19}F spectra.^{S1} The self-diffusion coefficient D was obtained by fitting the measured signal intensity I as a function of gradient strength g to the Stejskal-Tanner equation:^{S3}

$$I = I_0 e^{-D\gamma^2 g^2 \delta^2 (\Delta - \delta/3)} = I_0 e^{-Db} \quad (\text{S2})$$

where γ is the gyromagnetic ratio of the detected nucleus and b is the Stejskal-Tanner parameter.

The activation energy E_a was determined by measuring D as a function of temperature over 6 steps between 13 and 30°C. The sample was equilibrated for 20–40 min. between each temperature step. The temperature was maintained by flowing nitrogen gas at 270 L/h (triflic acid) or 400 L/h (PFSI) through a chiller (XR401 with TC-84 control unit, FTS Systems, Warminster, PA) and into the NMR probe, where the gas stream was heated to the appropriate temperature using the Bruker VT system. Sample temperatures were calibrated to $\pm 0.5^\circ\text{C}$ with ethylene glycol^{S4} that was either placed in the sealed membrane cell (PFSI measurements) or in a 5 mm NMR tube (triflic acid measurements). Error in D is estimated at $\pm 3\%$ and E_a error is estimated at $\pm 5\%$.

Results

Figure S1 shows representative diffusion and activation energy plots for H_2O in PFSI at water uptakes of $\lambda = 15.2$ and $\lambda = 2.1$. All activation energy plots showed distinctly Arrhenius behavior.

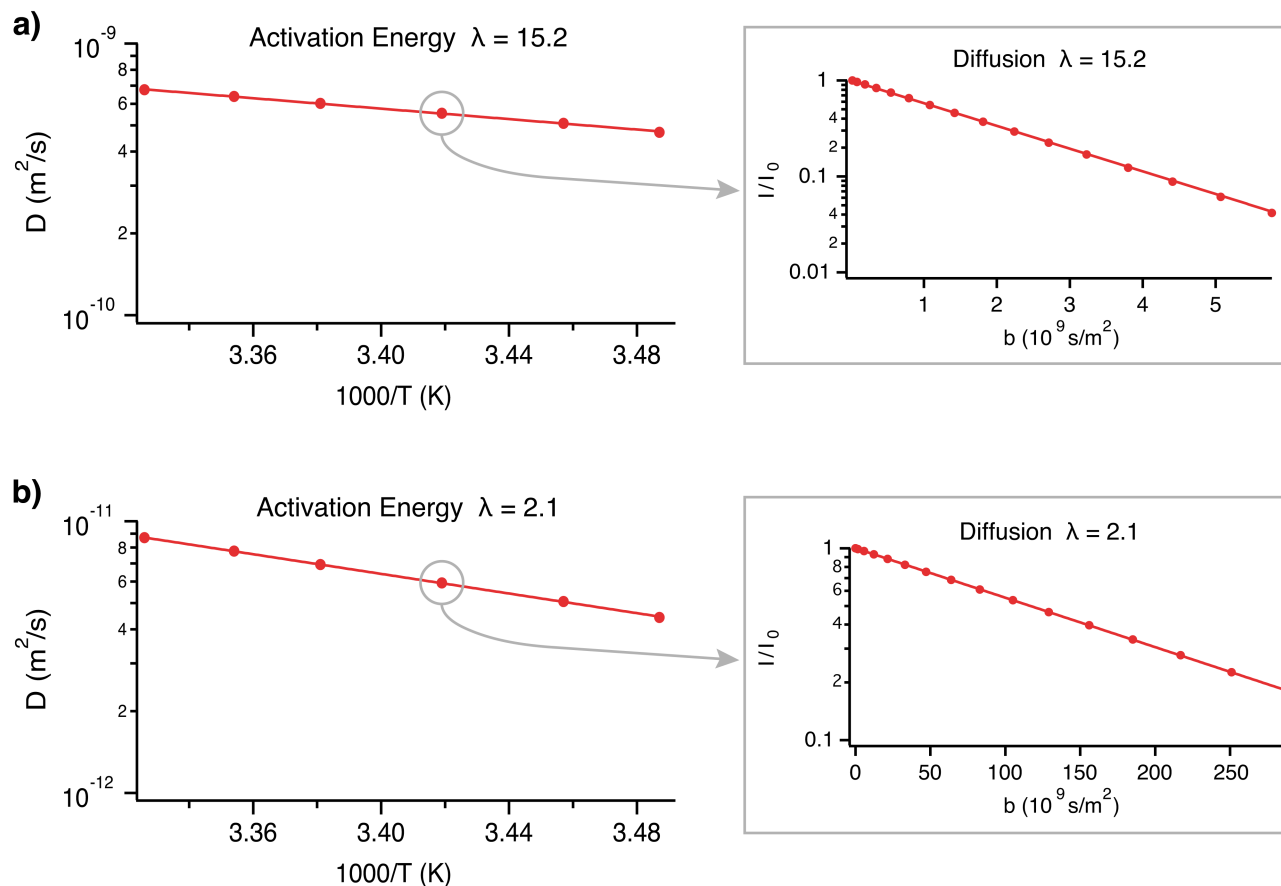


Fig. S1 Plots for calculating E_a , with insets showing determination of D at 19.3 °C. Two representative plots were chosen: (a) PFSI with H₂O uptake of $\lambda = 15.2$ and (b) PFSI at $\lambda = 2.1$. The Arrhenius plots are fit to Eq. 1 (main text) to give E_a and the pre-exponential factor D_0 . The diffusion decay plots are fit to Eq. S2 to give the self-diffusion coefficient D . Error bars on these plots are smaller than the symbol sizes.

In addition to the discussion of Figure 2 in the main text (Diffusion vs. water uptake), we also note that the diffusion of ²H₂O in PFSI is slightly slower than that of ¹H₂O. This is expected, given the 10 % slower diffusion of pure ²H₂O relative to pure ¹H₂O.^{S5}

Here we discuss several other points regarding our E_a data in Figure 3 (main text). First, the E_a of pure triflic acid is comparable to that of dilute triflic acid solutions. This implies that the solution structure that leads to higher triflic acid E_a values only occurs when some water is present to interact with the triflic acid. Second, there is no significant isotope effect for water absorbed in PFSI, as the E_a for ¹H₂O and ²H₂O were identical at both low and high hydration levels. E_a will only be correlated with fluctuations around the diffusing species, and if these species experience similar local energetic fluctuations, they will have similar E_a . Finally, we mention that while slower D measurements sometimes lead to a higher E_a , this is not a generally valid relationship. This can be seen in the dramatically different shapes of the D and E_a plots, and by observing how pure water diffuses faster than dilute triflate anions in solution, while the E_a values are nearly identical. The topological restrictions in the PFSI channel network, the diffusion measurement encoding times, and the local mechanisms of diffusion serve to weight the absolute values of the measured D .

Upon comparing our E_a results to those previously presented in the literature for Nafion PFSI, our values are higher by 3–10 kJ/mol. Ye *et al.*^{S6} used ¹H magic angle spinning (MAS) NMR linewidth measurements to calculate E_a values of 16.4 kJ/mol for dried Nafion 112 and 11 kJ/mol for hydrated Nafion. Kidena^{S7} used PFG-NMR diffusometry and found an anisotropic E_a between 13 and 16 kJ/mol for λ between 5.7 and 9.5 on Nafion 212. Cappadonia *et al.*^{S8} used impedance spectroscopy and found E_a values for Nafion 117 at six hydration levels, and our values are 5 – 10 kJ/mol higher at each point. The trend in these last data looks similar to our own, with a sharp decrease in E_a with increasing hydration until a certain hydration level where E_a reaches a plateau. As mentioned in the main text, the various E_a measurement techniques probe different local processes and give slightly different averages over H₂O, H₃O⁺, H₅O₂⁺, and other species. Measurements of E_a with PFG NMR give the E_a of all mobile hydrogen atoms in the system, summing the contributions from both water and acidic protons. Because of this, we expect PFG-NMR to give a higher E_a value than conductivity measurements or conceivably rotational measurements (solid state NMR), because the energy scale of proton transport (Grotthuss hopping mechanism weighted) should be somewhat lower in magnitude than that of water transport (vehicle mechanism weighted).^{S9} We also note that even at high hydration ($\lambda > 12$) E_a for the PFSI is 1-3 kJ/mol lower than pure water or the triflic acid solutions. This must be a result of the nanostructuring of the PFSI channels or effects of the polymer side chain or main chain motions within the channel. Even at high hydration, for example, the electrostatic environment in the middle of the channel will not be the same as in pure water. This will be the focus of further experiments and atomistic simulation studies. Regardless, our PFG-NMR measurements are self-consistent, and the conclusions drawn from our study lie in the relative changes in E_a and not necessarily from the absolute values of the measurements.

Figure S2 shows the measured pre-exponential factor D_0 as a function of λ . D_0 represents diffusion at infinite temperature and therefore reports on the configurational degrees of freedom available to the system, which in turn reflects the entropy of the system. The maximum D_0 value is observed at $\lambda \approx 3$ and $\lambda \approx 7$ for triflic acid and PFSI, respectively, which is nearly consistent with the critical λ values above which E_a is independent of hydration level. This indicates that the triflic acid-

water system has the largest degrees of freedom for transport in different pathways at $\lambda \approx 3$, and thus the most favorable cluster size is $\text{CF}_3\text{SO}_3\text{H}---(\text{H}_2\text{O})_3$. The higher D_0 maximum for PFSI ($\lambda \approx 7$) suggests that at lower hydration levels there are limited pathways for transport due to the configurationally restricted sidechains and clusters of SO_3^- groups. For both triflic acid and PFSI, increasing the hydration level above the D_0 maximum will cause the system to behave more like pure water and thus have a reduced number of possible configurations relative to the mixed system. This phenomenon is related to the positive entropy of mixing in (statistical) thermodynamic systems, and further discussion of D_0 will follow in future publications.

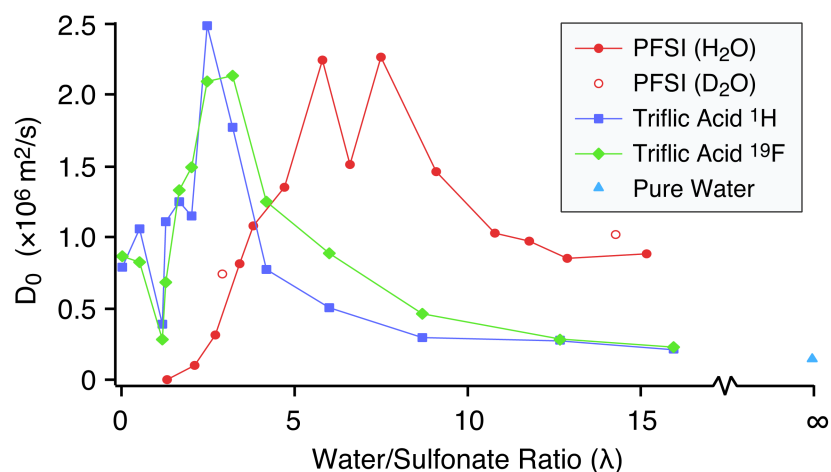


Fig. S2 Pre-exponential factor (D_0) of PFSI and triflic acid with varying hydration (λ). For the PFSI, values are given for both $^1\text{H}_2\text{O}$ and $^2\text{H}_2\text{O}$, and for triflic acid both ^1H and ^{19}F signals are measured. The D_0 for pure water is given at right. The error in D_0 is approximately $\pm 10\%$.

Discussion

Here we discuss the physical meaning of activation energy in non-solid systems. For rigid solids, the physical picture is clear: the E_a of diffusion is the energy barrier that must be overcome for a molecule to jump from its current lattice position to an adjacent lattice vacancy. However this picture does not cleanly apply to liquids or soft matter, where there are no fixed lattice or vacancies. Instead, there exists a dynamic phase of disordered molecules undergoing translational and rotational motion.

In order to explore the physical meaning of E_a , we can connect the diffusion coefficient (the phenomenological parameter) with fluctuations (non-equilibrium properties) using the fluctuation-dissipation theorem, which links the macroscopic relaxation rate to microscopic dynamics.^{S10} A schematic diagram of the microscopic process of diffusion is shown in Figure S3, where the path of an individual molecule is highlighted as diffusion occurs. Starting at $t = 0$, the molecule of interest begins to translate and collide with nearby molecules. As time proceeds and more collisions occur, the molecule of interest loses memory of its initial position and velocity. The time it takes for this to occur is known as the translational correlation time, τ_c , which describes how long a local molecule takes to reach equilibrium (uncorrelated motion) from an initial state. The collisions during the initial τ_c period remain correlated, describing the microscopic properties of diffusion. The Langevin model is used to describe the stochastic process of diffusion, correlating the friction force (macroscopic) and the fluctuation force (microscopic). The friction force is the systematic force that depends on the velocity of a probe molecule, and the fluctuation force is a random force that is velocity independent and correlated with collisions during τ_c . E_a , which is derived from thermally activated local molecular processes, is closely related to the fluctuation force, thereby characterizing the average energetics of collisions during τ_c .^{S10}

This concept indicates that E_a , which correlates with local fluctuations, does not have a direct relationship with the D , which is regulated by the friction force. The similar E_a values of ^1H in triflic acid solutions ($\lambda > 3$) and water inside PFSI ($\lambda > 8$) (Figure 3, main text) obtained from dramatically different diffusion coefficients (Figure 2, main text) validate that E_a characterizes local intermolecular interactions during τ_c and is not directly related to diffusion coefficient magnitudes. For diffusion of liquids, $\tau_c \sim 1$ ps and the lengthscale of this process is that of several molecules (< 1 nm). Therefore, measurements of E_a provide information on the average over all local interactions that occur on the pre-diffusional (~ 1 ps) timescale.

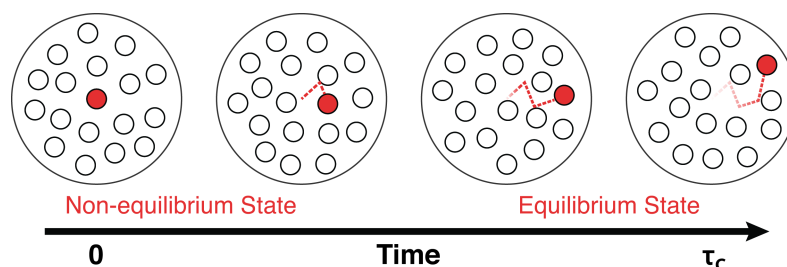


Fig. S3 Schematic of time and length scale of activation energy measurement in liquids. The solid circle represents the molecule of interest, starting from a snapshot at time zero and then undergoing random collisions. At a time represented by the translational correlation time, τ_c , the highlighted molecule no longer has a memory of its initial position and velocity. All molecular interactions in this correlated time period contribute to E_a .

Finally, we comment further on insights our measurements can provide into proton transport mechanisms. Generally, three types of proton transport are possible in ionic polymer membranes.^{S9} One is the vehicle mechanism, where the proton is transported by the diffusion of large species such as H_3O^+ . The second is the Grotthuss mechanism, where protons are transferred between adjacent water molecules in a ‘hopping’ fashion that is mediated by molecular reorganization. The third mechanism occurs when protons hop between two adjacent sulfonate groups via one or more water molecules, and this is called the surface conduction or surface diffusion mechanism. In PFSIs, it is thought that the relative prevalence of the mechanisms varies with water uptake.^{S9,S11} At high hydration, the ion channels are swollen to such an extent that the absorbed water behaves as in a dilute acid solution, where the Grotthuss mechanism dominates. At low hydration, the increase in charged species (including clustering) and decrease in configurational mobility of the sidechains disrupts the water structure and suppresses proton transfer, and proton transport occurs mainly through the vehicle and surface mechanisms.^{S9,S11} Eikerling *et al.*^{S11c} showed computationally that the activation energy of surface conduction is higher than that of proton hopping in the center of the channel, and thus the overall activation energy should decrease with increasing channel size (and thus hydration) up to a saturation point. Our measurements support this conclusion, with a saturation point at $\lambda \approx 7$. Future studies will explore the conduction effects arising from different types of water-proton species and the details of how E_a and D from PFG NMR probe these effects.

References

- S1 (a) J. Hou, J. Li and L.A. Madsen, *Macromolecules*, 2010, **43**, 347; (b) J. Li, K.G. Wilmsmeyer and L.A. Madsen, *Macromolecules*, 2009, **42**, 255.
- S2 T. A. Zawodzinski Jr, M. Neeman, L. O. Sillerud and S. Gottesfeld, *J. Phys. Chem.*, 1991, **95**, 6040.
- S3 E.O. Stejskal and J.E. Tanner, *J. Chem. Phys.*, 1965, **42**, 288.
- S4 C. Ammann, P. Meier and A.E. Merbach, *J. Magn. Reson.*, 1982, **46**, 319.

- S5 M. Holtz and H. Weingärtner, *J. Magn. Reson.*, 1991, **92**, 115.
- S6 G. Ye, N. Janzen and G.R. Goward, *Macromolecules*, 2006, **39**, 3283.
- S7 K. Kidena, *J. Membr. Sci.*, 2008, **323**, 201.
- S8 M. Cappadonia, J.W. Erning, S.M. Saberi Niaki and U. Stimming, *Solid State Ionics*, 1995, **77**, 65.
- S9 K.D. Kreuer, *Chem. Mater.*, 1996, **8**, 610
- S10 D. Chandler, *Introduction to Modern Statistical Mechanics*, Oxford University Press, USA, 1st edn., 1987.
- S11 (a) T.A. Zawodzinski, C. Derouin, S. Radzinski, R.J. Sherman, V.T. Smith, T.E. Springer and S. Gottesfeld, *J. Electrochem. Soc.*, 1993, **140**, 1041; (b) K.D. Kreuer, T. Dippel, W. Meyer and J. Maier, *J. Mater. Res. Soc. Symp. Proc.*, 1993, **293**, 273; (c) M. Eikerling, A.A. Kornyshev, A.M. Kuznetsov, J. Ulstrup and S. Walbran, *J. Phys. Chem. B*, 2001, **105**, 3646.